Amyloidogenic light chains induce cardiomyocyte contractile dysfunction and apoptosis via a non-canonical p38α MAPK pathway

Jianru Shi[a], Jian Guan[a,b], Bingbing Jiang[a], Daniel A. Brenner[a], Federica del Monte[c], Jennifer E. Ward[d], Lawreen H. Connors[d], Douglas B. Sawyer[e], Marc J. Semigran[f], Thomas E. Macgillivray[g], David C. Seldin[b,d], Rodney Falk[h], and Ronglih Liao[a,b,1]

[a]Cardiac Muscle Research Laboratory, Cardiovascular Division, Department of Medicine, Brigham and Women's Hospital, Harvard Medical School, Boston, MA 02115; [b]Molecular Medicine Graduate Program and [d]Amyloid Treatment and Research Program, Boston University School of Medicine, Boston, MA 02118; [c]Cardiovascular Institute, Beth Israel Deaconess Medical Center and Harvard Medical School, Boston, MA 02215; [e]Division of Cardiovascular Medicine, Department of Medicine, Vanderbilt University School of Medicine, Nashville, TN 37232; [f]Cardiac Unit and [g]Cardiac Surgical Division, Massachusetts General Hospital, Boston, MA 02114; and [h]Harvard Vanguard Medical Associates, Boston, MA 02116

Patients with primary (AL) cardiac amyloidosis suffer from progressive cardiomyopathy with a median survival of less than 8 months and a 5-year survival of <10%. Contributing to this poor prognosis is the fact that these patients generally do not tolerate standard heart failure therapies. The molecular mechanisms underlying this deadly form of heart disease remain unclear. Although interstitial amyloid fibril deposition of Ig light chain proteins is a major cause of cardiac dysfunction in AL cardiac amyloidosis, we have previously shown that amyloid precursor proteins directly impair cardiac function at the cellular and isolated organ levels, independent of fibril formation. In this study, we report that amyloidogenic light chain (AL-LC) proteins provoke oxidative stress, cellular dysfunction, and apoptosis in isolated adult cardiomyocytes through activation of p38 mitogen-activated protein kinase (MAPK). AL-LC–induced p38 activation was found to be independent of the upstream MAPK kinase, MKK3/6, and instead depends upon transforming growth factor-β-activated protein kinase-1 binding protein-1 (TAB1)-mediated p38α MAPK autophosphorylation. Treatment of cardiomyocytes with SB203580, a selective p38 MAPK inhibitor, significantly attenuated AL-LC–induced oxidative stress, cellular dysfunction, and apoptosis. Our data provide a unique mechanistic insight into the pathogenesis of AL-LC cardiac toxicity and suggest that TAB1-mediated p38α MAPK autophosphorylation may serve as an important event leading to cardiac dysfunction and subsequent heart failure.

amyloid | cell death | heart failure | TAB1 | reactive oxygen species

The amyloidoses represent a group of protein misfolding diseases that share a common pathology of extracellular fibril deposition. Amyloidoses can be either localized or systemic diseases (1, 2). Primary amyloidosis, now termed AL (amyloidogenic Ig light chain) amyloidosis, is the most common form of systemic amyloidosis in the United States. AL amyloidosis is distinguished by the clonal production of Ig light chain proteins and subsequent multiorgan amyloid deposition and dysfunction (2, 3). More than 50% of AL amyloidosis patients suffer from cardiac involvement, developing a rapidly progressive form of cardiomyopathy and heart failure with a medium survival of less than 8 months and a 5-year survival of less than 10% (4). Patients with AL cardiac amyloidosis generally do not tolerate standard heart failure medications including digoxin, β-blockers, and angiotensin converting enzyme inhibitors. Despite recent advances in diagnostic and treatment modalities, prognosis with AL cardiac amyloidosis remains exceedingly poor, highlighting the importance of elucidating the underlying mechanisms and identifying novel therapeutic strategies for this group of patients.

Our previous work has challenged the long-standing notion that interstitial amyloid fibril deposition is the sole cause for cardiac dysfunction. Using isolated cardiomyocytes and heart preparations, we have demonstrated that amyloidogenic Ig light chain proteins (AL-LC) directly cause oxidative stress and dysfunction independent of fibril deposition (5, 6). These observations agree with the concept that amyloid precursor proteins, not amyloid fibrils, cause organ dysfunction and contribute to the pathophysiology and progression in various amyloid-related diseases (7, 8). Among the multiple key mediators involved in the regulation of redox status, stress-responsive p38 mitogen-activated protein kinases (MAPK) have been reported to be activated in other types of amyloid disease such as Alzheimer's disease (9–12). Our prior findings have implicated oxidative stress in AL-LC–induced cellular dysfunction. We, therefore, set out to determine whether p38 MAPK could be an important mediator in the pathogenesis of AL-LC–induced cardiac dysfunction.

Herein, using human light chain proteins isolated from patients with AL cardiomyopathy and nonamyloid myeloma patients, we demonstrate that p38 MAPK is immediately and differentially activated by AL-LC but not by light chains obtained from nonamyloid myeloma patients (Con-LC). We further discover that the AL-LC–induced p38 MAPK activation is not mediated via canonical MAPK kinases but rather through a recently identified novel p38α autophosphorylation mechanism (13, 14). Importantly, inhibition of p38 MAPK by either the selective inhibitor SB203580 or overexpression of a dominant negative p38α, but not a dominant negative p38β, prevented AL-LC–induced oxidative stress, cardiomyocyte dysfunction, and apoptosis, suggesting that activation of p38α through autophosphorylation may play a pivotal role in triggering AL-LC–induced cellular dysfunction and potentially contribute to the subsequent pathogenesis of AL cardiac amyloidosis.

Results

Isolation of Human AL-LC Proteins. AL-LC used in the experiments were isolated and purified from urine specimens collected from patients referred to the Amyloid Research and Treatment Program at Boston University School of Medicine. To complement our experimental group, we employed two essential controls for all our experiments: vehicle control (vehicle) and nonamyloid

control light chain (Con-LC) proteins isolated from patients with multiple myeloma. A brief summary of the types of LC and clinical symptoms of the patients when the samples were collected are detailed in Table S1.

AL-LC Activates p38 MAPK in Isolated Adult Cardiomyocytes. Our previous findings have indicated that AL-LC increases oxidative stress in isolated cardiomyocytes and suggested that redox-sensitive signaling pathways may be involved in AL-LC–induced cellular dysfunction. Therefore, we measured phosphorylation levels of p38, JNK, and ERK in isolated adult rat cardiomyocytes treated with AL-LC (20 μg/mL), Con-LC (20 μg/mL), or vehicle (ultrapure water). Immunoblot analysis showed that there was a relatively low basal level of p-p38, p-JNK, and p-ERK in isolated adult cardiomyocytes. Fifteen minutes exposure of isolated cardiomyocytes to AL-LC significantly enhanced p38 phosphorylation as compared to Con-LC and vehicle-treated cells (Fig. 1A), without affecting the phosphorylation state of ERK and JNK (Fig. 1A). A time course revealed that the phosphorylation of p38 by AL-LC occurred as early as 5 min, peaked at 15 min, and then returned to basal levels in 60 min (Fig. 2B). To test whether AL-LC–induced p38 MAPK activation was specific to protein isolated from one human sample, we examined p38 phosphorylation after exposure of cardiomyocytes to seven other AL-LC and one more Con-LC. We observed elevated p38 phosphorylation in all eight AL-LC treated, but not in Con-LC-treated cardiomyocytes (Fig. 1C). These data suggest that activation of p38 MAPK may represent an initial event mediating AL-LC effects on isolated cardiomyocytes.

Inhibition of p38 MAPK Activation Prevents AL-LC–Induced Cardiomyocyte Dysfunction. To test our hypothesis that p38 acti-vation mediates AL-LC–induced cardiomyocyte dysfunction, we treated cardiomyocytes with AL-LC, Con-LC, or vehicle in the absence or in the presence of 5 μM SB203580, a selective p38 MAPK inhibitor, and examined reactive oxygen species (ROS) production and cell contractility. AL-LC but not Con-LC significantly enhanced ROS production as determined by increased DCF (dichloroflorocine) fluorescence, a fluorescent dye sensitive to H_2O_2, (Fig. 2A), and significantly impaired cardiomyocyte contractility as revealed by reduced percent cell shortening (%CS) (Fig. 2B) measured by an edge detection technique (6). Strikingly, inhibition of p38 MAPK by SB203580 completely prevented AL-LC–induced ROS production (Fig. 2A) and impairment of cell contractility (Fig. 2B). These data strongly support the notion that activation of p38 MAPK pathway plays a critical role in AL-LC–induced oxidative stress and cardiomyocyte dysfunction.

AL-LC Induces TAB1-Mediated p38 Autophosphorylation. We next examined whether AL-LC may activate MKK3/6, well-known p38 MAPK upstream kinases. Immunoblot using antibody against phosphorylated MKK3/6 revealed a basal level of phosphorylation in vehicle-treated cells. However, the phosphorylation state of MKK3/6 was unchanged with AL-LC treatment (Fig. 3A), strongly suggesting that AL-LC–induced p38 activation is via MKK3/6-independent mechanisms.

Emerging data suggest that TAB1 may recruit activated p38, which can result in p38 autophosphorylation. This pathway serves an alternative means for p38 MAPK to be phosphorylated/activated in a noncanonical fashion under certain conditions (13, 15). Note that in contrast to upstream MKK-mediated p38 MAPK phosphorylation, autophosphorylation requires p38 MAPK intrinsic kinase activity. We therefore
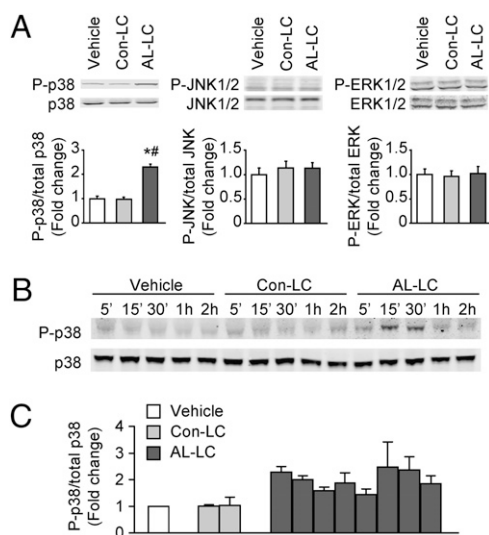
Fig. 1. AL-LC activates p38 MAPK in isolated adult rat cardiomyocytes. (A) Immunoblots showing phospho- and total p38, JNK, and ERK MAPKs in isolated cardiomyocytes incubated with vehicle, Con-LC (20 μg/mL), or AL-LC (20 μg/mL) for 15 min. Bar graphs summarize the data from three independent experiments, with vehicle control set as 1-fold. *, P < 0.05 vs. vehicle; #, P < 0.05 vs. Con-LC. (B) Phosphorylation of p38 in cardiomyocytes under the same treatment conditions as above for designated times. Immunoblots are representatives of two separate experiments. (C) Bar graph summarizing the ratio of phospho- to total p38 expression in cardiomyocytes incubated for 15 min with Con-LC and AL-LC isolated from two myeloma patients (code no.: 96–100 and 00–161) and eight AL patients (code no.: 00–131, 00–127, 01–003, 99–145, 00–112, 01–091, 02–131, and 01–052), respectively, with vehicle control set as 1-fold. The experiments were repeated three times. Detailed information for the human samples is summarized in Table S1.
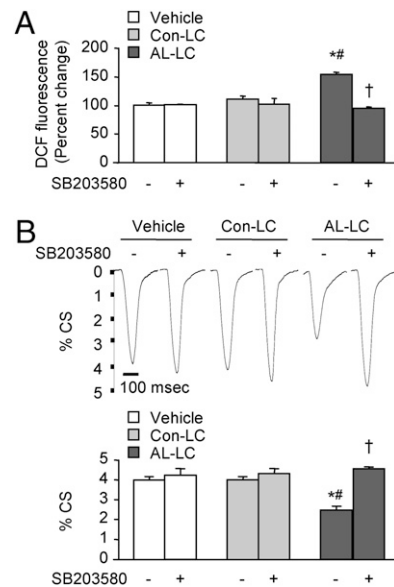
Fig. 2. Pharmacological inhibition of p38 MAPK activity prevents AL-LC–induced oxidant stress and contractile dysfunction in isolated adult cardiomyocytes. Inhibition of p38 MAPK with SB203580 (5 μM) attenuated AL-LC–induced reactive oxygen species (ROS) production as determined by DCF fluorescence (A) and contractile dysfunction indicated by the decreased percent cell shortening (%CS) as measured by edge detection methodology (B). Bar-graph data are from three independent experiments. For B, data are means ± SE from three independent experiments, with each individual experiment average values taken from 8 to 12 cell measurements for each group. Representative tracings of single cell shortening at respective conditions are displayed above the bar graph. *, P < 0.05 vs. vehicle and #, P < 0.05 vs. Con-LC in the presence or absence of SB203580; †, P < 0.05 vs. AL-LC in the absence of SB203580.

CELL BIOLOGY
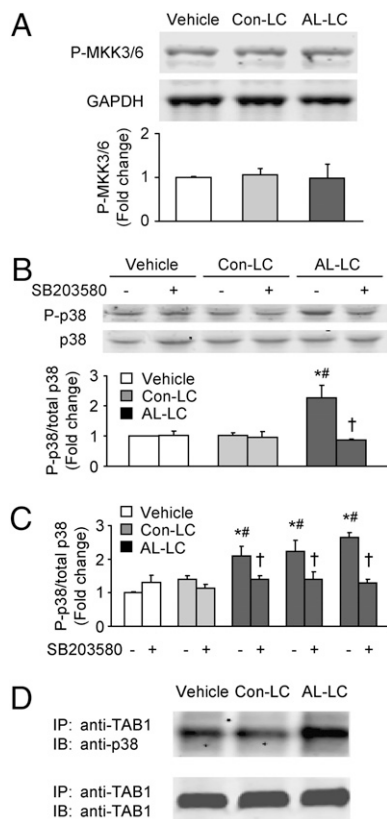
Fig. 3. AL-LC activates p38 MAPK via autophosphorylation but not MKK3/6 activation. (A) Immunoblot shows no difference in MKK3/6 phosphorylation among the cardiomyocytes incubated with vehicle, Con-LC (20 μg/mL), or AL-LC (20 μg/mL) for 15 min. (B) AL-LC–induced p38 phosphorylation was inhibited in cardiomyocytes by SB203580 (5 μM) that was added 30 min before the addition of vehicle, Con-LC, or AL-LC. (C) The inhibition of AL-LC–induced p38 phosphorylation was further demonstrated with three more AL-LC isolated from AL patients (code no.: 01–052, 00–112, and 02–131). The experimental conditions were the same as described in B. (D) Co-IP assay on isolated cardiomyocytes incubated with vehicle, Con-LC, or AL-LC for 15 min demonstrated an increased interaction of p38 MAPK and TAB1 after incubation with AL-LC. Cardiomyocyte extract IP with anti-TAB1 antibody was followed by immunoblotting with anti-p38 antibody (Upper) and anti-TAB1 antibody (Lower, served as loading control). Each bar graph data are from three independent experiments. *, $P < 0.05$ vs. vehicle and #, $P < 0.05$ vs. Con-LC in the presence or absence of SB203580; †, $P < 0.05$ vs. AL-LC in the absence of SB203580.

examined whether inhibition of p38 MAPK activity by SB203580 could abolish p38 MAPK phosphorylation induced by AL-LC. As shown in Fig. 3B, the enhancement of p38 MAPK phosphorylation by AL-LC treatment was significantly attenuated by the presence of SB203580 (5 μM); however, inhibition of p38 MAPK activity by SB203580 did not change the basal level of p38 phosphorylation, suggesting that constitutive activation of MKK3/6 may contribute to the basal level of p38 MAPK activation that is independent of AL-LC–triggered p38 MAPK phosphorylation. We further tested three additional AL-LC from AL patients described in Table S1 and observed a similar inhibitory effect of SB203580 on AL-LC–induced p38 MAPK phosphorylation (Fig. 3C). Using immunoprecipitation of TAB1 with TAB1-specific antibody from total cell lysate followed by immunoblotting with anti-TAB1 and anti-p38 antibodies, we found an increase in endogenous TAB1 and p38 MAPK interaction in cells treated with AL-LC in comparison with Con-LC and vehicle-treated groups (Fig. 3D). Taken together, these results suggest that TAB1-mediated p38 autophosphorylation

rather than canonical p38 MAPK activation is an early event in AL-LC–induced cellular stress and dysfunction.

Activation of p38α, but not p38β, Contributes to AL-LC–induced Impairment of Cardiomyocyte Contractility. Recent data have suggested that p38α but not p38β is capable of associating with TAB1 for autophosphorylation (16). To further dissect the role of p38 autophosphorylation in mediating the AL-LC–induced cardiomyocyte stress and dysfunction, we infected cardiomyocytes with adenoviruses overexpressing LacZ, dominant negative p38α (p38αDN), or dominant negative p38β (p38βDN) for 24 h (Fig. 4A) followed by exposure to vehicle, Con-LC, or AL-LC. In agreement with the data obtained from the inhibition of p38 MAPK by SB203580, overexpression of p38αDN completely prevented AL-LC–induced impairment of cell shortening (Fig. 4B). In contrast, overexpression of LacZ or p38βDN did not render any protection to AL-LC–induced cellular dysfunction (Fig. 4B). These data provide unambiguous evidence that the activation of p38α but not p38β plays a predominant role in mediating the deleterious effect of AL-LC on cardiomyocyte contractility.

AL-LC Induces Cardiomyocyte Apoptosis Through Activation of p38α MAPK. Emerging evidence suggests that excess ROS production and TAB1-mediated p38α autophosphorylation may lead to cellular apoptosis (17, 18). Therefore, we examined whether AL-LC–induced p38α autophosphorylation might induce cardiomyocyte apoptosis. Using a TUNEL assay, we observed a significantly higher percentage of TUNEL positive cells in cardiomyocytes treated with AL-LC for 48 h than those in Con-LC or vehicle groups (Fig. 5 A and 5B), suggesting a strong cytotoxic effect of AL-LC. The AL-LC–induced cell apoptosis was substantially inhibited by the presence of either antioxidant MnTMPyP (50 μM) (Fig. 5A) or SB203580 (5 μM) (Fig. 5B). Consistent with the TUNEL data, immunoblot analysis of Bax and Bcl2 protein expression showed that AL-LC enhanced Bax expression but reduced Bcl2 expression, leading to an increased Bax/Bcl2 ratio. Similarly, the increase in Bax to Bcl2 ratio was prevented by treatment with SB203580 (Fig. 5C). Furthermore, AL-LC–induced apoptosis was prevented by overexpression of p38αDN, but not by overexpression of LacZ or p38βDN (Fig.
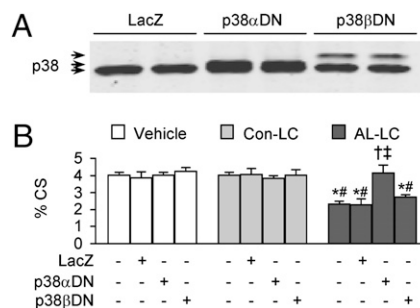
Fig. 4. AL-LC–induced cellar dysfunction is prevented by adenovirus mediated overexpression of dominant negative p38α but not dominant negative p38β. (A) Immunoblot of total p38 MAPK expression in isolated adult cardiomyocytes infected with adenovirus (MOI of 50) expressing LacZ, dominant negative p38α (p38αDN), or dominant negative p38β (p38βDN). Arrows indicate endogenous p38 (Lower), p38αDN (Middle), and p38βDN (Upper), respectively. (B) Overexpression of p38αDN, but not p38βDN, prevents AL-LC–induced contractile dysfunction in isolated cardiomyocytes as shown by percent cell shorting. Data are means ± SE from three independent experiments, with each individual experiment average values taken from 8 to 12 cell measurements for each group. * and #, $P < 0.05$ vs. corresponding vehicle and control-LC, respectively; † and ‡, $P < 0.05$ vs. AL-LC–treated cells overexpressing LacZ and without adenovirus infection, respectively.

Fig. 5. AL-LC activates programmed cell death through a p38α MAPK-dependent mechanism. (A) Increased apoptosis as determined by TUNEL assay in isolated cardiomyocytes incubated with AL-LC for 48 h relative to vehicle or Con-LC treatment. Coincubation of AL-LC with MnTMPyP (50 μM), a MnSOD mimetic, reduced cellular apoptosis. (B) AL-LC–induced apoptosis was prevented by inhibition of p38 MAPK with SB203580 (5 μM). (C) AL-LC enhanced Bax/Bcl2 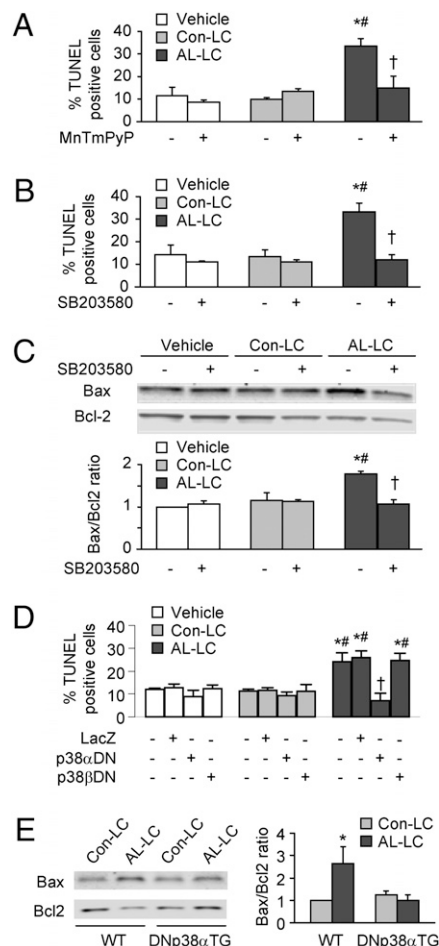expression ratio, which was prevented by treatment with SB203580. (D) AL-LC–induced apoptosis was inhibited by adenovirus-mediated overexpression of dominant negative p38α (p38αDN) but not dominant negative p38β (p38βDN). Bar graph data are means ± SE, each from three independent experiments. * and #, $P < 0.05$ vs. corresponding vehicle and Con-LC, respectively; †, $P < 0.05$ vs. AL-LC treated cells without MnTmPyP (A), SB203580 (B and C), as well as with vehicle or LacZ (D). (E) i.v. administration of AL-LC for 7 days increased cardiac tissue Bax/Bcl2 expression ratio in wild-type (WT) mice but not in DNp38αTG mice. n = 3 for each group, *, $P < 0.05$.

5D), supporting a distinct role for p38α in mediating AL-LC–induced apoptotic signaling pathways.

AL-LC Induces p38α MAPK-Dependent Apoptosis in Vivo. To determine whether AL-LC induces programmed cell death in cardiac tissue in vivo, LC were introduced into wild type (WT) and transgenic mice with cardiac-specific overexpression of dominant negative p38α (DNp38αTG) by initial tail vein injection (300 μg of LC per mouse) followed by systemic i.v. infusion via osmotic minipump (420 μg of LC infused per mouse over 7 days). Infusion of AL-LC in WT mice resulted in an increase in the Bax/Bcl2 ratio as determined by Western blot analysis (Fig. 5E) in the hearts relative to Con-LC infusion, as well as an increase in cellular apoptosis as determined by TUNEL staining (Fig. S1). Cellular apoptosis was independent of amyloid fiber deposition,

as evidenced by the lack of any Congo Red staining in AL-LC hearts. Importantly, similarly to as observed in vitro in a cell culture system, in vivo AL-LC–induced apoptosis was prevented in mice overexpressing p38αDN MAPK (Fig. 5E and Fig. S1). Taken together, our data suggest that AL-LC–induced apoptosis occurs in vivo after short-term exposure to circulating LC and is mediated by p38α MAPK-dependent mechanisms.

Increased Apoptosis in Heart Tissue from Patients with AL Cardiomyopathy. To determine whether apoptosis also is present in humans with AL cardiomyopathy, we measured apoptosis in human heart tissues obtained by biopsy from six nonfailing human hearts and four hearts from patients with AL cardiomyopathy (AL). Consistent with what we observed in our in vitro rat cardiomyocyte model and in vivo in mice, a significantly higher percentage of TUNEL-positive cells was observed in the AL group compared with nonfailing hearts (Non-FH) (Fig. 6A). In addition, caspase 3/7 activity was significantly higher in AL samples compared to Non-FH samples (Fig. 6B), as was Bax/Bcl2 expression and an increase in p53 expression (Fig. 6 C and D). Our data suggest an involvement of apoptosis in human AL cardiomyopathy.

Discussion

AL amyloidosis, the most common form of systemic amyloidosis, frequently results in cardiac involvement with impairment of diastolic and, eventually, systolic function. When present, cardiac dysfunction rapidly leads to symptomatic heart failure and death. To date, treatment options are limited for patients with AL cardiac amyloidosis, as a lack of understanding of the fundamental molecular basis of this disease, in part, has precluded the development of effective agents. Clinical observations have suggested that patients with AL cardiac amyloidosis who achieve hematologic remission (defined as normalization of circulating free light chain levels) with anti-plasma cell chemotherapy improve in terms of heart failure symptoms, in spite of minimal or no change in echocardigraphically measured wall thickness. These clinical observations have led to the concept that monoclonal Ig light chain proteins directly provoke cytotoxicity in cardiomyocytes, in addition to the damage caused by extrac-
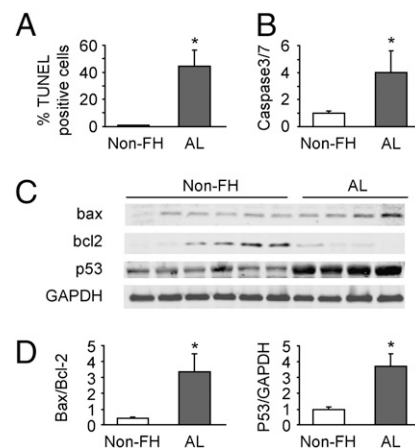
Fig. 6. Increased apoptosis is observed in explanted human myocardium obtained from patients with primary cardiac amyloidosis as compared to myocardium obtained from nonfailing human hearts. Nonfailing heart (Non-FH) samples (n = 6) were obtained from NDRI and explanted AL heart samples (n = 4) were obtained from patients with AL cardiac amyloidosis undergoing cardiac transplantation. Apoptosis was evaluated by TUNEL assay (A), caspase3/7 activity (B), and ratio of Bax/Bcl2 protein expression and p53 expression normalized with GAPDH (C and D). Corresponding immunoblots of Bax, Bcl2, p53, and GAPDH are shown in C, where GAPDH serves as a loading control. Data are presented as means ± SE. *, $P < 0.05$ vs. Non-FH.

CELL BIOLOGY

ellular deposition of amyloid. This clinical observation is concordant with our data that AL-LC alone can induce oxidative stress and cellular dysfunction in isolated cardiomyocytes and hearts (5, 6). In this study, we reveal that human AL-LC rapidly and differentially activates TAB1-mediated p38α phosphorylation in isolated adult cardiomyocytes. More importantly, the activation of this stress activated protein kinase leads to subsequent redox stress, cellular dysfunction, and apoptosis, which can be prevented by inhibition of p38 via pharmacological inhibitors and/or adenovirus mediated gene transfer of dominant negative p38. It is noteworthy that the rapid activation of p38 by AL-LC has been confirmed with AL-LC isolated from eight AL patients, thus substantiating the significance of our findings.

The p38 MAPK signaling pathway is known to play a critical role in cell stress response, apoptosis, cytoskeletal reorganization, and transcriptional regulation of genes involved in differentiation, proliferation, and inflammation (19, 20). The p38 MAPK contains four family members, p38α, p38β, p38γ, and p38δ, and all share a conserved Thr-Gly-Tyr (TGY) dual-phosphorylation motif in the activation loop that can be phosphorylated by upstream MAPK kinases (MAPKK). Activation of p38 MAPK is thought to be mediated by a cascade of phosphorylation events involving upstream MAPKK, such as MKK3 and/or MKK6, as well as further upstream MAPKK kinases, such as TAK1 and ASK1 (21, 22). This mechanism, by far, is the most widely studied and recognized canonical means to phosphorylate and activate p38 MAPK. Recently, alternative pathways to activate p38 MAPK via the intermolecular autophosphorylation that can be initiated by either T cell antigen receptor (TCR) (23) or the scaffold protein TAB1 have been reported (13). Interestingly, we observed increased p38 MAPK phosphorylation occurred within a time frame in which MKK3/6 were not activated. These data led us to question the mode of p38 phosphorylation in isolated cardiomyocytes under the context of AL-LC–mediated activation.

It is known that the activities of p38α and p38β can readily be inhibited by a selective p38 MAPK inhibitor, SB203580. SB203580 exerts its inhibitory effect by binding to the ATP binding pocket of p38 MAPK, thus inhibiting its ability to undergo autophosphorylation, but not affecting the capacity of p38 MAPK to be phosphorylated by upstream MAPKK, MKK3/6. Taking advantage of this chemical property, SB203580 has been used to identify the p38 MAPK autophosphorylation in cultured cells in several prior published studies (13–15, 17, 24). In this report, we found that AL-LC–induced p38 phosphorylation was SB203580-sensitive and that TAB1–p38 interaction was dramatically increased in cells treated with AL-LC, suggesting that AL-LC–augmented p38 phosphorylation occurs through TAB1-mediated autophosphorylation. The involvement of TAB1-mediated autophosphorylation was further supported by evidence that overexpression of a dominant negative p38α MAPK prevented elevated ROS, cardiomyocyte contractile dysfunction, and apoptosis induced by AL-LC, whereas overexpression of a dominant negative p38β MAPK had no significant effect. This result is consistent with the notion that the noncanonical TAB1-mediated pathway targets only p38α MAPK but not p38β MAPK for autophosphorylation (13, 16). Whether TAB1-mediated and MKK3/6-mediated p38 MAPK activation may have different functions due to the involvement of different p38 MAPK isoforms remains unclear. However, emerging evidence suggests that activation of p38α MAPK, either through MKK3/6-mediated phosphorylation or through TAB1-mediated autophosphorylation, may be particularly critical in inducing cellular apoptosis, whereas activation of p38β may have an opposite role (13–15, 17, 24–26). Moreover, specifically targeting p38α for activation by AL-LC through a noncanonical pathway in cardiomyocytes may change the functional balance of different p38 MAPK isoforms and may, ultimately, lead to cell dysfunction and death.

Although other amyloid precursor proteins or oligomers, most notably Aβ from Alzheimer's disease, have been shown to activate a programmed cell death pathway and contribute to the pathology of the disease state, our data demonstrates that AL-LC from patients with primary amyloidosis can also trigger such programmed cell death. Moreover, our data show that AL-LC–induced cardiomyocyte apoptosis is associated with an increase in the Bax/Bcl2 expression ratio. Blocking of p38 MAPK activity with the pharmacological inhibitor, SB203580, effectively prevented the change in Bax/Bcl2 ratio. Heart samples from patients with primary cardiac amyloidosis provided further evidence to support the involvement of Bax/Bcl2 ratio change in apoptosis in heart tissues. We do, however, recognize that the potential caveats associated with using explanted human heart tissue, despite the significant efforts put forth to ensure the quality and consistency of the human samples obtained. Nonetheless, these results are consistent with previous reports by others (26), suggesting that the p38α MAPK autophosphorylation may trigger cell apoptosis by differentially regulating the expression and/or activities of pro- and anti-apoptotic Bcl2 family proteins. Given that the inhibition of p38 MAPK activity by SB203580 prevented excess ROS generation induced by AL-LC and that an antioxidant MnTMPyP rescued cardiomyocytes from apoptosis, it is clear that ROS are involved in the AL-LC–induced p38 MAPK signaling cascade, eventually leading to cell apoptosis. Additionally, AL-LC–induced cellular apoptosis was observed in vivo in mice after delivery of LC into the systemic circulation via osmotic pump for 7 days and, importantly, these effects were prevented in mice with cardiac-specific overexpression of dominant negative p38α. These in vivo data suggest the exciting possibility of using p38α specific inhibitors for the treatment for AL cardiomyopathy. Further studies investigating the detailed molecular events underlying the AL-LC–induced cardiac dysfunction/cell death and the functional significance of TAB1-mediated p38α MAPK autophosphorylation in vitro and in vivo are certainly needed.

In summary, our data suggest that triggering p38α MAPK autophosphorylation plays a crucial role in amyloidogenic Ig light-chain mediated cellular oxidative stress, dysfunction and ultimately cell death in cardiomyocytes. Because cardiac involvement is the major determinant predicting clinical outcomes in patients with AL amyloidosis, our findings represent a major step forward toward revealing the molecular mechanisms underlying AL cardiac amyloidosis and could contribute to the development of early diagnosis and treatment strategies for this group of patients with very limited medical options.

Materials and Methods

Light Chain Isolation and Purification. Ig light chain proteins were isolated from 24-h urine samples obtained from the patients with primary amyloidosis referred to the Amyloid Treatment and Research Program at Boston University School of Medicine, as well as from patients with multiple myeloma, as described (5). All samples were collected with informed consent and approved by Institutional Review Board at Boston University School of Medicine.

Rat Cardiomyocyte Isolation and Culture. Ventricular cardiomyocytes were isolated from 150- to 180-g male Wistar rats (Charles River Laboratories) by using collagenase perfusion method detailed (27). Isolated cardiomyocytes were cultured overnight before the incubation with vehicle (ultrapure water), 20 μg/mL of Con-LC or AL-LC for designated times for each assay. All procedures associated with handling of animals were approved by Institutional Animal Care and Use Committee.

Measurement of Intracellular ROS. Intracellular ROS levels were determined by using the cell-permeable, redox-sensitive fluorophore, dichlorofluorescein-diacetate (DCF-DA) (Invitrogen) (6). After 24 h of incubation with vehicle, Con-LC, or AL-LC, the cardiomyocytes were incubated with 20 μM DCF-DA for 30 min and DCF fluorescence was visualized using Nikon (TS100) fluorescence microscopy and analyzed with SigmaScan Pro-4.0.

Measurement of Cell Contractility. Cell contractility was measured in cultured adult cardiomyocytes as described (27). Briefly, after incubation with vehicle, Con-LC or AL-LC for 24 h, cardiomyocytes were perfused with Tyrode solution containing 1.2 mM Ca^{2+} at 37 °C and field stimulated at a frequency of 5 Hz. Cell shortening/relengthening was measured by using video edge detection (IonOptix, Milton, MA). %CS was calculated as the difference between diastolic and systolic cell lengths normalized to the diastolic cell length.

Human Samples. Nonfailing human heart samples (*n* = 6) with no evidence of cardiac disease were obtained from National Disease Research Interchange (NDRI) and explanted AL heart samples (*n* = 4) were obtained from patients with primary cardiac amyloidosis undergoing cardiac transplantation at Massachusetts General Hospital (for additional information, see Table S2). All tissues from donor and transplant patients were collected in cold and oxygenated Wisconsin cardioplegic solution immediately after harvest. All procedures related to human tissue were reviewed and approved by Institution Review Board (IRB) committee at Massachusetts General Hospital.

Statistical Analysis. All quantitative data are presented as means ± SE. Statistical analysis was performed by ANOVA, and a *P* value <0.05 was considered to be significant.

Other Materials and Methods. Culture medium, antibodies, adenoviruses, immunoprecipitation, Western blot analysis, TUNEL assay, Caspase 3/7 activity assay, and in vivo LC infusion are detailed in SI Methods.

1. Merlini G, Bellotti V (2003) Molecular mechanisms of amyloidosis. *N Engl J Med* 349: 583–596.
2. Falk RH, Comenzo RL, Skinner M (1997) The systemic amyloidoses. *N Engl J Med* 337: 898–909.
3. Westermark P, et al. (2002) Amyloid fibril protein nomenclature—2002. *Amyloid* 9: 197–200.
4. Falk RH (2005) Diagnosis and management of the cardiac amyloidoses. *Circulation* 112:2047–2060.
5. Liao R, et al. (2001) Infusion of light chains from patients with cardiac amyloidosis causes diastolic dysfunction in isolated mouse hearts. *Circulation* 104:1594–1597.
6. Brenner DA, et al. (2004) Human amyloidogenic light chains directly impair cardiomyocyte function through an increase in cellular oxidant stress. *Circ Res* 94: 1008–1010.
7. Schubert D, et al. (1995) Amyloid peptides are toxic via a common oxidative mechanism. *Proc Natl Acad Sci USA* 92:1989–1993.
8. Walsh DM, et al. (2002) Naturally secreted oligomers of amyloid beta protein potently inhibit hippocampal long-term potentiation in vivo. *Nature* 416:535–539.
9. Hensley K, et al. (1999) p38 kinase is activated in the Alzheimer's disease brain. *J Neurochem* 72:2053–2058.
10. Oddo S, et al. (2005) Chronic nicotine administration exacerbates tau pathology in a transgenic model of Alzheimer's disease. *Proc Natl Acad Sci USA* 102:3046–3051.
11. Origlia N, et al. (2008) Receptor for advanced glycation end product-dependent activation of p38 mitogen-activated protein kinase contributes to amyloid-beta-mediated cortical synaptic dysfunction. *J Neurosci* 28:3521–3530.
12. Lambourne SL, et al. (2005) Increased tau phosphorylation on mitogen-activated protein kinase consensus sites and cognitive decline in transgenic models for Alzheimer's disease and FTDP-17: evidence for distinct molecular processes underlying tau abnormalities. *Mol Cell Biol* 25:278–293.
13. Ge B, et al. (2002) MAPKK-independent activation of p38alpha mediated by TAB1-dependent autophosphorylation of p38alpha. *Science* 295:1291–1294.
14. Tanno M, et al. (2003) Diverse mechanisms of myocardial p38 mitogen-activated protein kinase activation: Evidence for MKK-independent activation by a TAB1-associated mechanism contributing to injury during myocardial ischemia. *Circ Res* 93: 254–261.
15. Lu G, et al. (2006) TAB-1 modulates intracellular localization of p38 MAP kinase and downstream signaling. *J Biol Chem* 281:6087–6095.
16. Zhou H, et al. (2006) Determinants that control the specific interactions between TAB1 and p38alpha. *Mol Cell Biol* 26:3824–3834.
17. Fiedler B, et al. (2006) cGMP-dependent protein kinase type I inhibits TAB1-p38 mitogen-activated protein kinase apoptosis signaling in cardiac myocytes. *J Biol Chem* 281:32831–32840.
18. Nojiri H, et al. (2006) Oxidative stress causes heart failure with impaired mitochondrial respiration. *J Biol Chem* 281:33789–33801.
19. Kyriakis JM, Avruch J (2001) Mammalian mitogen-activated protein kinase signal transduction pathways activated by stress and inflammation. *Physiol Rev* 81:807–869.
20. Baines CP, Molkentin JD (2005) STRESS signaling pathways that modulate cardiac myocyte apoptosis. *J Mol Cell Cardiol* 38:47–62.
21. Wang Y (2007) Mitogen-activated protein kinases in heart development and diseases. *Circulation* 116:1413–1423.
22. Johnson GL, Lapadat R (2002) Mitogen-activated protein kinase pathways mediated by ERK, JNK, and p38 protein kinases. *Science* 298:1911–1912.
23. Round JL, et al. (2007) Scaffold protein Dlgh1 coordinates alternative p38 kinase activation, directing T cell receptor signals toward NFAT but not NF-kappaB transcription factors. *Nat Immunol* 8:154–161.
24. Li J, Miller EJ, Ninomiya-Tsuji J, Russell RR, 3rd, Young LH (2005) AMP-activated protein kinase activates p38 mitogen-activated protein kinase by increasing recruitment of p38 MAPK to TAB1 in the ischemic heart. *Circ Res* 97:872–879.
25. Makeeva N, Roomans GM, Welsh N (2007) Role of TAB1 in nitric oxide-induced p38 activation in insulin-producing cells. *Int J Biol Sci* 3:71–76.
26. Ren J, Zhang S, Kovacs A, Wang Y, Muslin AJ (2005) Role of p38alpha MAPK in cardiac apoptosis and remodeling after myocardial infarction. *J Mol Cell Cardiol* 38:617–623.
27. Jain M, et al. (2003) Glucose-6-phosphate dehydrogenase modulates cytosolic redox status and contractile phenotype in adult cardiomyocytes. *Circ Res* 93:e9–e16.

CELL BIOLOGY